The Influence of Activity on Axon Pathfinding in the Optic Tectum

Elizabeth M. Kita,[1] Ethan K. Scott,[2] Geoffrey J. Goodhill[1,3]

[1] Queensland Brain Institute, The University of Queensland, Brisbane, Australia

[2] School of Biomedical Sciences, The University of Queensland, Brisbane, Australia

[3] School of Mathematics and Physics, The University of Queensland, Brisbane, Australia

Received 12 August 2014; revised 22 December 2014; accepted 23 December 2014

ABSTRACT: **The relative importance of neural activity versus activity-independent cues in shaping the initial wiring of the brain is still largely an open question. While activity is clearly critical for circuit rearrangements after initial connections have been made, whether it also plays a role in initial axon pathfinding remains to be determined. Here, we investigated this question using the guidance of zebrafish retinal ganglion cell axons to their targets in the tectum as a model. Recent results have implicated biased branching as a key feature of pathfinding in the zebrafish tectum. Using tetrodotoxin to silence neural activity globally, we found a decrease in the area covered by axon branches during pathfinding. After reaching the target, there were dynamic differences in axon length, area and the number of branches between conditions. However, other aspects of pathfinding were unaffected by silencing, including the ratio of branches directed toward the target, length, and number of branches, as well as turning angle, velocity, and number of growth cones per axon. These results challenge the hypothesis that neural connections develop in sequential stages of molecularly guided pathfinding and activity-based refinement. Despite a maintenance of overall guidance, axon pathfinding dynamics can nevertheless be altered by activity loss.** Develop Neurobiol 75: 608–620, 2015

Keywords: **neural development; topographic maps; retinal ganglion cell; axon pathfinding; time-lapse; tetrodotoxin; zebrafish; tectum**

INTRODUCTION

The role of neural activity in shaping brain structure is a critical question in neuroscience. Patterned activity is well known to affect the refinement of connections once axons have reached their targets (reviewed in Kirkby et al., 2013), but whether it also affects the initial guidance of axons to those targets is unknown. There is evidence both for and against this hypothesis. Pulses of electrical activity can increase the responses of axons to attractive cues and convert repulsion into attraction in vitro (Ming et al., 2001), which suggests that activity could potentially help guide the turning responses of growth cones in vivo. The loss of neural activity during development also leads to regional mistargeting and disruptions to patterned layering in the cortex (Catalano and Shatz, 1998), and imbalances of activity between the two cortical hemispheres can lead to defects of callosal axon guidance (Suàrez et al., 2014). Conversely, general patterns of connections can persist despite activity loss in mammals (Sretavan et al., 1988), chick (Kobayashi et al., 1990), axolotl (Harris, 1984), and fish (Kaethner and Stuermer, 1994; Gnuegge et al.,

Correspondence to: G. J. Goodhill (g.goodhill@uq.edu.au)

Contract grant sponsor: National Health and Medical Research Council (NHMRC project grant 1043044, G.J.G. and E.K.S.) an International Postgraduate Research Scholarship (E.M.K.) and Queensland Brain Institute (E.M.K.).

Published online 22 January 2015 in Wiley Online Library (wileyonlinelibrary.com).
DOI 10.1002/dneu.22262

2001), although the connections later fail to refine into precisely connected circuits (e.g., Ruthazer et al., 2003; Xu et al., 2011; Rodger et al., 2012). There is increasing support for the idea that activity and biochemical mechanisms cooperate during brain development (reviewed in Ruthazer and Cline, 2004; Spitzer, 2006; Garel and López-Bendito, 2014). However, many important questions remain unanswered.

The retinotectal projection is an important model addressing the contributions of activity to axon guidance in vivo. In zebrafish, this pathway is near the surface of the brain and easily visualized during development. Axons from the retinal ganglion cells (RGCs) traverse the midline to the contralateral tectum. At the tectum, they grow through the neuropil to a target area where they establish a terminal arbor. These arbors form a topographic map which preserves the spatial relationships between the positions of their cell bodies in the retina and dendritic receptive fields in the tectum (Kita et al., 2014). Maintaining this map during continued retinal and tectal growth requires ongoing synaptic plasticity. While the tectum and retina generate new cells along mismatched axes (e.g., Gaze et al., 1979; Reh and Constantine-Paton, 1984; McLoon, 1985; Fraser and O'Rourke, 1990) RGC axonal arbors rearrange their branches and synaptic structures to compensate.

Early evidence suggested that in fish, growth cones guide axons directly to their targets between 3 and 5 days post fertilization (dpf) (Stuermer, 1988; Kaethner and Stuermer, 1992). However, recent results have shown that dynamic branches are present during the targeting phase, and that growth cones extend in straight trajectories after initiation rather than turning toward the target (Simpson et al., 2013). The branches are selectively initiated or stabilized to decrease the distance to the eventual zone of arborization, creating more branches pointing toward the target direction than away (Simpson et al., 2013). There is a high rate of turnover in branches over the pathfinding period, similar to periods of later plasticity occurring after 5 dpf.

An important unanswered question in this past work is whether axonal branching dynamics during the pathfinding phase are affected by early neural activity. Similarities between the dynamics of branching during pathfinding and during rearrangement suggest that previous insights into branch control during rearrangement may apply to pathfinding as well. However, work investigating the role of neural activity in branch rearrangement has produced conflicting results. For individual arbors, blocking activity decreases the length and number of branches after 5 dpf (Gnuegge et al., 2001). Suppressing activity increases the rate of branch extensions and retractions measured at 6–7 dpf (O'Rourke et al., 1994; Fredj et al., 2010). In contrast, silencing can also cause smaller and less complex arbors to form, and decreases the mobility of axons and their branches as early as 5 dpf (Hua et al., 2005). It thus was not obvious what effect activity might have on the biased branching mechanism of initial pathfinding (from 2.5 to 4 dpf) identified by Simpson et al. (2013).

Here we investigated this question by injecting tetrodotoxin (TTX) into developing zebrafish. We explored the role of neural activity in pathfinding by taking detailed measurements every 10 min for up to 44 h and quantifying the changes to the pathfinding behavior in single RGC axons as they traveled across the tectum to their target. We found that the area explored by axon branches during pathfinding was decreased after TTX injections. The remaining dynamics of pathfinding were similar to controls, and in particular the biased branching during pathfinding was maintained despite of the loss of activity. Growth cone turning angles were also similar between both groups. These data show that global activity contributes to the initial guidance to the target in this system but is not necessary for overall pathfinding.

MATERIALS AND METHODS

Breeding and Raising

Adult zebrafish were raised by The University of Queensland Biological Resources Aquatics team. Fish were kept on a 14/10 h light/dark cycle. Embryos were obtained by timed matings between zebrafish carrying a variegated BGUG (*Brn3c:GAL4;UAS:mGFP)* transgene (Scott et al., 2007) and Atoh7:GAL4 transgenic fish. Embryos developed in E3 buffer media (5 m*M* NaCl, 0.17 m*M* KCl, 0.33 m*M* $CaCl_2$, and 0.33 m*M* $MgSO_4$) supplemented with 0.00003% methylene blue (30 ppm) for the first 24 h. After this point, E3 with 200 μ*M* (0.003%) PTU (N-phenylthiourea, Sigma Aldrich) was used to disrupt pigment formation for clear imaging (Karlsson et al., 2001). BGUG expressing embryos were screened out from the crosses to obtain larvae with a low density of fluorescently labeled RGCs. All procedures were performed with approval from The University of Queensland Animal Ethics Committee (in accordance with approvals SBMS/362/10/NHMRC, IMB/181/13/BREED and IBC/777/SBMS/2012).

TTX Injections

At 54 hpf, embryos were anaesthetized in 0.016% tricaine (MS-222) dissolved in E3. The embryos were then mounted in 1.5% low melting point SeaPlaque Agarose (Lonza).

TTX powder (Sigma-Aldrich) was dissolved in milliQ H2O with 110 μL of 20 m*M* citrate to create a 1 m*M* TTX solution. Phenol red was added to the injected aliquots for visibility. TTX travels throughout the entire larva at this stage and results in paralysis (Stuermer and Raymond, 1989; Gnuegge et al., 2001). To avoid damage to the retinotectal system, we injected 4.5–9 nL of 1 m*M* TTX into the yolk rather than into the eye or the tectum as has previously been described (Stuermer et al., 1990; Gnuegge et al., 2001). Control fish were injected in a similar fashion with E3 and phenol red. After injection, embryos were carefully removed from the agar and allowed to recover in E3 media at 28.5°C for 1–6 h. For the TTX treated group, injected embryos were paralyzed except for their heartbeats and did not respond to touch. Any embryo responding to touch was discarded. Paralysis was an initial indicator of successful TTX treatment. Previous studies have shown that zebrafish injected with TTX at 30–36 hpf remain both silenced and paralyzed until 150 hpf (Stuermer et al., 1990) and we observed movement returning to the fish after a similar length of time.

Measuring Activity

To test neural activity levels after TTX injection, we imaged melanophore deficient "nacre" zebrafish (Lister et al., 1999) expressing a pan-neuronal calcium indicator GCaMP5 (Park et al., 2000; Akerboom et al., 2012) expressed as a transgenic Gal4:HuC; UAS:GCaMP5 reporter line (Scott lab). Images were rapidly streamed (10 Hz) from a spinning disk confocal microscope (inverted Zeiss Axio Observer Z1 utilizing a W1 Yokogawa spinning disk module and a Hamamatsu Flash4.0 sCMOS camera, controlled by Sildebook 5.5 software, 40× C-Apochromat lens 1.2 W Korr UV—VIS—IR, ∞/1.14–1.19). The 488 nm laser was used to record changes in fluorescence over time. The tectal neuropil displayed activity from both the entering RGCs and the recipient tectal cell dendrites and, since the TTX permeated the embryos, the tectal neuropil was a readout for activity in both the RGCs and the tectal cells. Analysis of the image series was done in ImageJ. The fractional changes in fluorescence over baseline levels ($\Delta F/F0$) were calculated as in Akerboom et al. (2012). Regions of interest (ROIs) were chosen along the anterior, posterior, central, medial, and lateral margins of the tectal neuropil, avoiding cell bodies. The fluorescence of each ROI was measured over 100 frames (10 s) isolated from 90 second movies from six fish in each condition, imaged over two consecutive days postinjection. $\Delta F/F$ was determined by dividing frames showing activity by frames where no activity was observed. If no activity was observed, 100 early frames were compared against 100 later frames as a background. Movies where the background fluorescence showed unusual slow rises in fluorescence or bleaching were excluded from the analysis.

Time-Lapse Imaging

Larvae bearing sparsely labeled RGCs were mounted in 1.5% low melting point agar (SeaPlaque; Lonza) as previously described (Simpson et al., 2013). The axons were imaged using a Plan-Apochromat 20× / 0.8 M27 objective on a Zeiss LSM 510 inverted confocal microscope with an incubation chamber set to 28.5°C. Stacks of up to 60 μm were taken through the developing tectum every 10 min using a 488-nm laser set at 7.5% power and using a BP 505–530 filter. Pinhole diameter was kept to 150 μm. The microscope contained a motorized stage allowed multiple fish to be mounted in the same dish and imaged concurrently. The imaging ran for up to 44 h continually, with axons growing in to the tectum at variable points during the time-lapse. For analysis, images were flattened into maximum intensity projections using Zen imaging software, as the arbors on the tectum are mostly planar (Fredj et al., 2010). The movies were exported as audio video interleave files (AVIs) and adjusted for brightness and contrast in ImageJ to ensure the axons were clearly visible. Ten individual axons were chosen from each condition for quantification. Each axon was aligned with respect to the time they stopped moving forward, defining the arrival at target ($t = 0$).

Time-Lapse Analysis

Researchers were blinded to treatment groups before analyses were performed. Custom Matlab (Mathworks) programs were used to isolate individual axons growing into the tectum. A semiautomated tracing process obtained the branch skeleton structure of the axon. The Manual Tracking plugin for ImageJ was used to follow the trajectories of growth cones. Data were then loaded into Matlab for quantitative analysis. A detailed description of the functions of the analysis program has been published previously (Simpson et al., 2013). For statistical analyses, the normality of sample distributions was first tested using the Shapiro–Wilks test. For normal distributions the built-in "ttest" (for one sample) or "ttest2" (for unpaired two-sample comparisons) functions in Matlab were used to determine *p*-values, allowing for potentially unequal variances of the two populations. When the sample distributions were not normal, the Mann–Whitney U test ("ranksum" in Matlab) was used to determine if there was a statistical difference. When multiple comparisons were made, as for over time-series, a Bonferroni correction was used.

Whole-Mount Immunochemistry

After the time-lapse movies were completed, fish were freed from the agar and anaesthetized in 0.02% tricaine (MS-222). Fish were then fixed in 4% paraformaldehyde (PFA) for 2.5 h at room temperature. The fixed tissues were then washed thoroughly in phosphate buffered saline (PBS) and permeabilized using 1 mg/mL collagenase for 1.5 h at room temperature. Primary antibodies detecting monoclonal acetylated tubulin raised in mice (Sigma, #T7451) and rabbit anti-GFP (Millipore, #AB3080P) were added at a concentration of 1:1000 in PBS + 0.2% Triton-X-100 overnight at 4°C. Primaries were washed out and secondaries Alexa Fluor 555 goat-anti-mouse (Life Technologies, A-

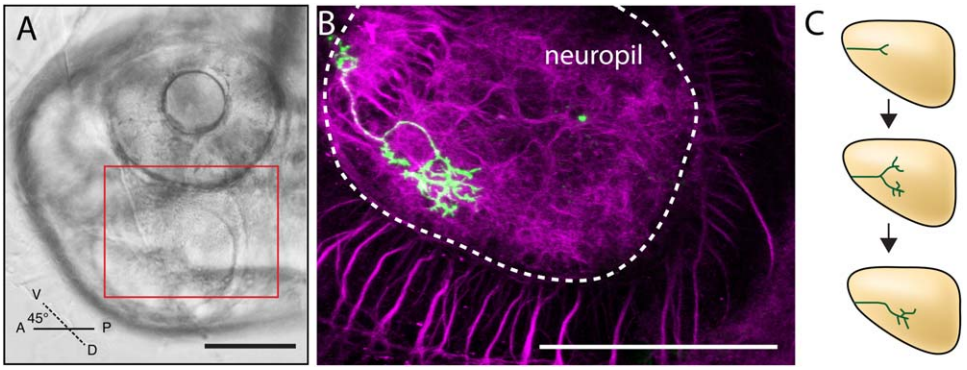

Figure 1 Imaging RGC growth on the tectum. (A) Brightfield view of a 54 hpf, PTU-treated zebrafish mounted in agar, dorsal side down and at a 45° angle to position the tectum close to the lens for inverted microscopy. The red rectangle marks the optic tectum and the approximate area imaged during pathfinding. (B) Confocal image of a fixed and immunostained whole mount after imaging at 5.5 dpf. An axon (mGFP, green) has arborized in the neuropil (dotted white outline). Only the right tectal neuropil is visible, with the arbor coming from a RGC in the left eye (out of frame). Anti-acetylated tubulin (magenta) allowed the architecture of the area to be visualized. (C) Schematic summarizing the mechanism identified by Simpson et al. (2013) for guidance by biased branching. Branches are extended and retracted dynamically during pathfinding, with more branches extending toward the target at any given time. Branches that decrease the distance to the target could become the primary axon shaft when other branches are retracted. Sequential rounds of branching refine the direction of travel, and this iterative process continues until the target is reached. Scale bars are 100 μm. A; anterior, D; dorsal, P; posterior, V; ventral.

11018) and Alexa Fluor 488 donkey-anti-rabbit (Life Technologies, A10040) were added at 1:500 and left overnight with rotation at 4°C. The fixed and immunostained samples could then be imaged to determine the final target area against the extent of the tectal surface. Brightness and contrast of each channel was adjusted in ImageJ for clear visibility.

RESULTS

We imaged axon pathfinding across the tectum [Fig. 1(A)]. Each axon travelled to a retinotopic location on the tectum before arborizing (Fig. 1(B)). Simpson et al. (2013) showed that zebrafish RGC axons display biased branching during pathfinding to their target zone (schematized in Fig. 1(C)). We asked whether the biased extension or stabilization of branches may be informed, at least partially, by early activity in the retinotectal system.

TTX successfully blocked action potentials in both the retina and the tectum when injected into the yolk of a developing zebrafish (Fig. 2). Gal4:HuC; UAS:GCaMP5 transgenic larvae were used to visualize calcium levels representing neural activity. As cellular responsiveness in the periventricular layers of the tectum differed among controls, we chose to use regions of the neuropil for analysis as it reliably displayed activity. In control animals at 4 and 5 dpf, the tectal neuropil exhibited frequent spontaneous activity [traces in Fig. 2(C,D)]. Diffuse blue light from the 488 nm laser also drove tectal activity for a few seconds in the superficial neuropil as previously described (Sumbre and Poo, 2013). Control fish displayed this response, and spontaneous activity was often observed in the neuropil afterwards. After TTX had been injected, the neuropil did not show spontaneous activity or any response to the laser light turning on. Usually activity (a sharp increase of $\Delta F/F$) occurred in medial or lateral regions in controls, and less often in the extreme anterior or posterior regions. In 1000 control frames, 6 events with $\Delta F/F$ were observed spanning 44 frames. No events were observed in 1000 frames from TTX treated fish (representative traces in Fig. 2(E)) ($n = 6$ zebrafish, 30 sampling areas). The inhibition of activity was still apparent 32 h after injection at 5 dpf (Fig. 2(F)).

For imaging the dynamics of growing axons, variegated BGUG fish were mounted in agar and injected with TTX or E3 at 54 hpf. Controls and TTX treated embryos were taken from the same clutch. The fish were imaged from 2.5 to 4.5 dpf. The resulting time-lapse movies of axon growth appeared similar by eye for TTX treated and control axons (Fig. 3).

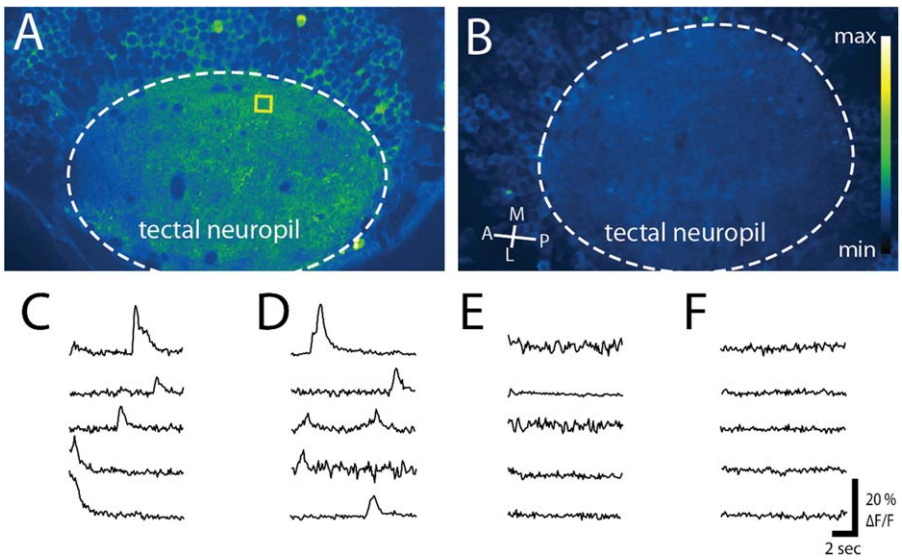

Figure 2 TTX reduced both spontaneous and induced activity in the tectal neuropil. (A,B) Images of the tectal neuropil in HuC:GCaMP5 fish at 4 dpf when injected (A) with a control (vehicle alone) or (B) TTX. 250 frames of each movie were stacked for maximum intensity over time and psuedo-colored with an imageJ Look Up Table (Green Fire Blue) where yellow shows the most intense activity over a blue background. (C, D) Spontaneous activity, as well as activity induced by the initiation of the 488 nm laser, was observed in the tectal neuropil in control cases at (C) 4 dpf and (D) 5 dpf. (E, F) When injected with TTX at 3.5 dpf no spiking activity was observed in the neuropil at (E) 4 dpf or (F) 5 dpf. Yellow box in (A) shows an example of a 25 × 25 pixel region chosen for activity analysis. A; anterior, M; medial, P; posterior, L; lateral.

Aspects of axon growth were quantitatively measured. One of the more interesting growth patterns was the biased branching, measured by the branch ratio in each frame. The branch ratio was defined in terms of the number of branches pointing toward the target (T) and the number of branches pointing away (A) at each time point by $(T - A)/(T + A)$. The branch ratios over time for individual control and TTX axons are shown in Figure 4(A,B). The branch ratios were similar between TTX and control groups ($n = 10$ axons, Fig. 4(C,D)). Both groups had tightly balanced rates of addition and deletion of branches between movie frames (Fig. 4(E)).

To compare the two groups quantitatively, each individual axon's branch ratio over time was fit to a straight line. Both lines had similar slopes representing the change in the branch ratio over the entire time-lapse sequence (TTX -0.04 ± 0.04 h-1, Controls -0.02 ± 0.03 h-1, $p = 0.21$) (Fig. 4(F)). Each of the groups also had similar branch ratios at time zero when their targets were reached (TTX 0.005 ± 0.10, Controls -0.07 ± 0.12, $p = 0.14$) [Fig. 4(F), first four measures]. The mean of the branch ratio for each axon was then calculated for two developmental

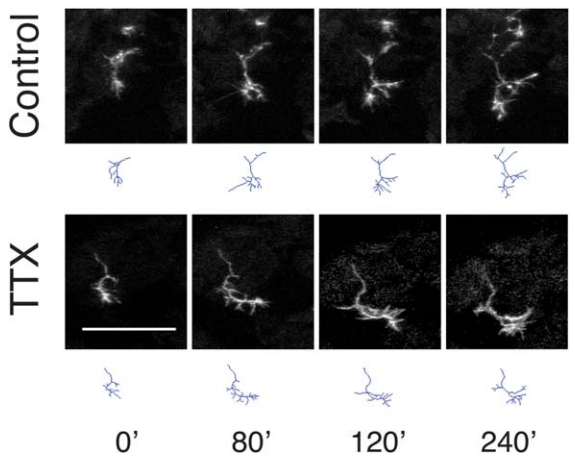

Figure 3 In control conditions and after treatment with TTX, axon growth appeared grossly similar. In individual frames taken from time-lapse movies, fish treated with control injections of E3 showed similar patterns of axon growth to embryos treated with TTX. There were no changes obvious by eye in target seeking behavior, branching or growth cone appearance. Tracings are shown below movie frames. Scale bar is 25 μm. Time is shown in minutes.

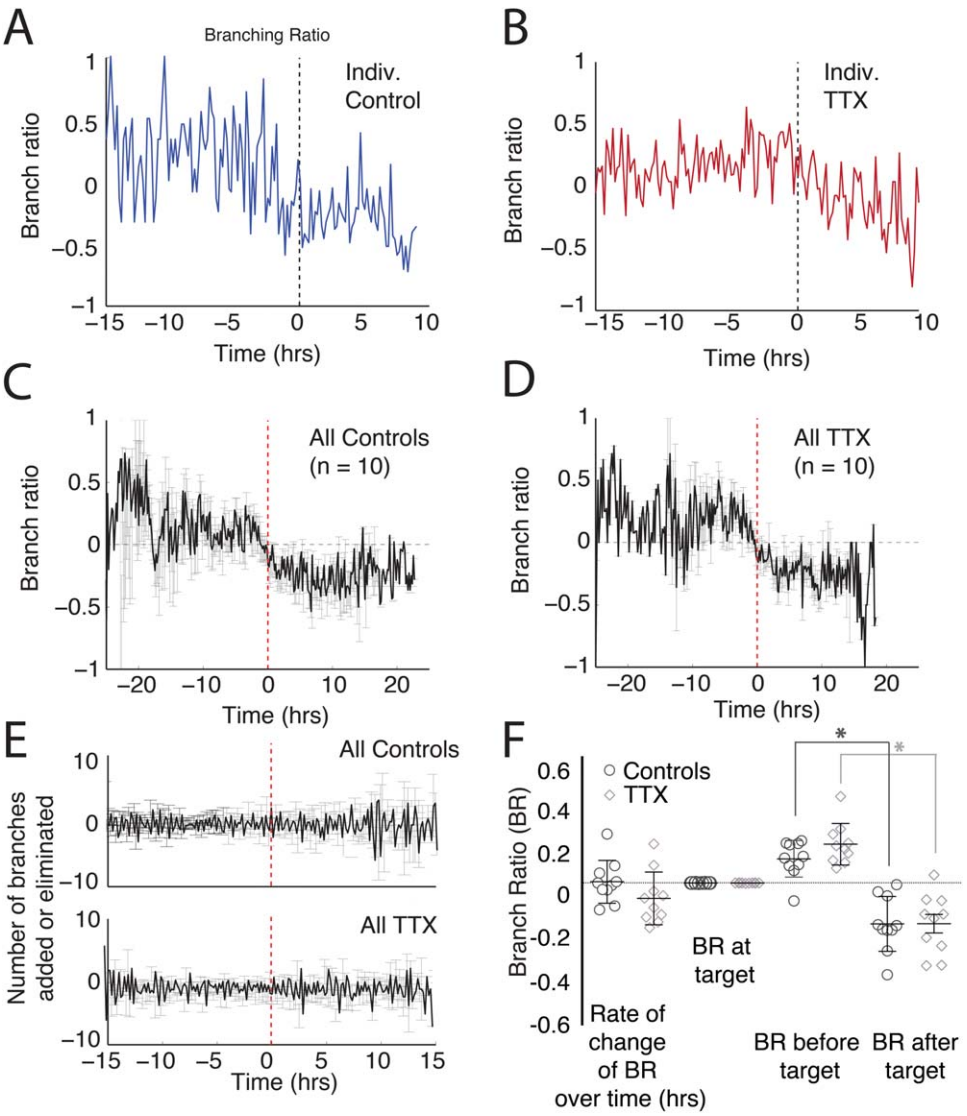

Figure 4 Guidance mechanisms were not altered by activity loss. (A, C, E(upper)) show measurements from control axons while (B, D, E(lower)) show axons after injection of TTX at 54 hpf. (A, B) Individual axon branch ratios were high during pathfinding and decreased when the target was reached. (C, D) For groups of 10 axons in each condition, the average branch ratio changed from positive to negative at the target. Axons were aligned to each other when they arrived at their targets, designated time 0. (E) Adding TTX did not change the number of branches added or eliminated in the 10 min periods. The number of additions and deletions remained tightly balanced in both cases. (F) The branch ratio showed a similar rate of change over the time-lapse movies, decreasing slowly for both controls and TTX. When the axons reached their target at $t = 0$ there was no significant difference between the branch ratios of control and TTX treated axons. Both control axons and those in the TTX condition had an overall positive ratio before the target was reached, and a significantly different and negative branch ratio after they reached their targets, but no differences were found in the measures of the branch ratio after treatment with TTX. Data points show averages of each axon. Controls; open circles, TTX; grey open diamonds, bar and whiskers display the mean ± SEM, *; $p < 0.001$.

stages: before hitting the target zone (pathfinding) and after (arborization). Overall, before reaching the target zone the branch ratio was positive and similar between the two groups (TTX 0.18 ± 0.10, Controls 0.11 ± 0.09, $p = 0.11$). After reaching the target, the branch ratios turned equivalently negative

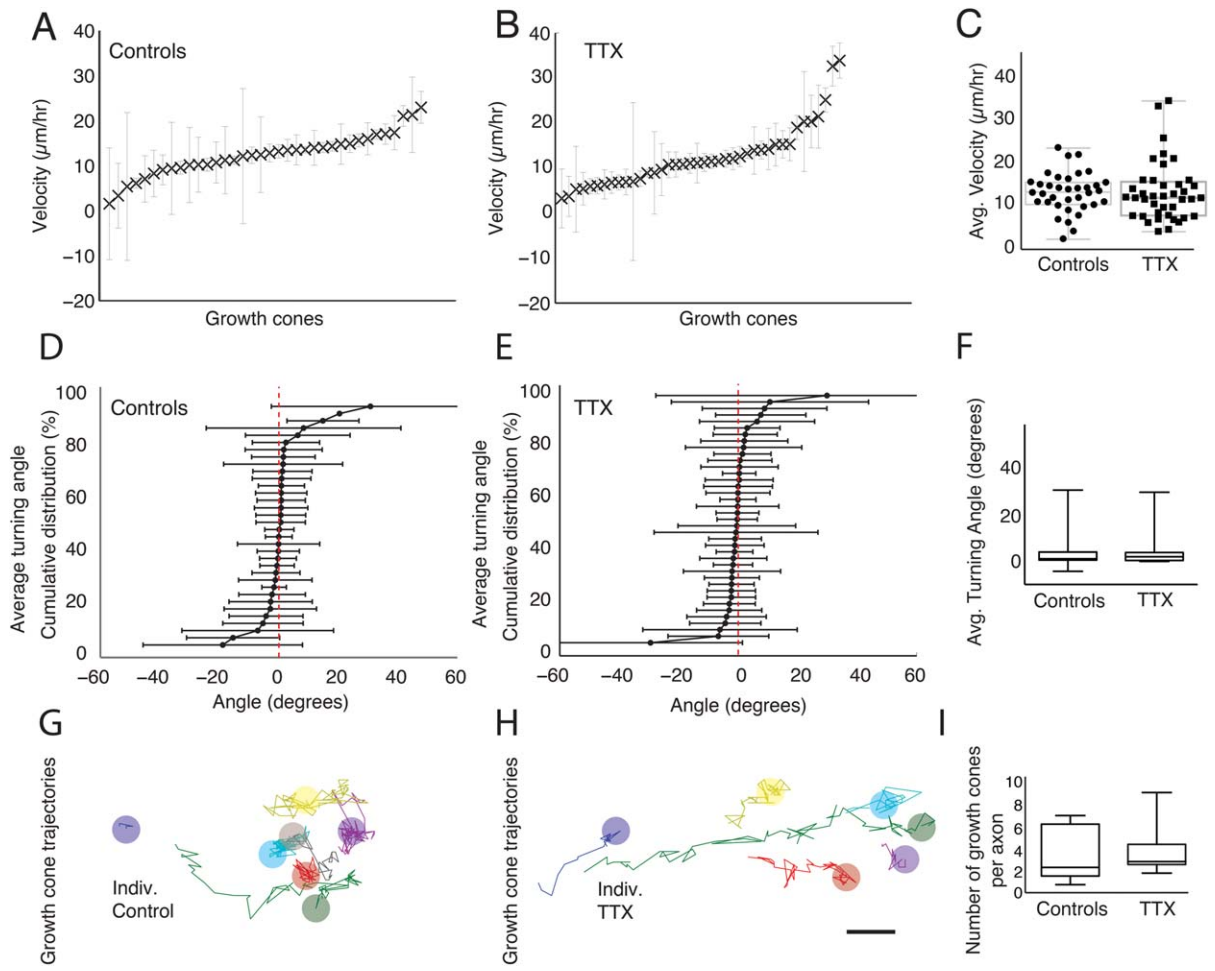

Figure 5 The average growth cone velocity, turning angle and trajectory were not altered by TTX. (A) Control and (B) TTX treated growth cones travelled at similar velocities. (C) There was no statistical difference between the average speeds of growth cones originating in normal or silent neural environments. Data points show averages of each growth cone, box and whisker plots are overlaid in grey. (D, E) The average turning angle for growth cones in each condition are shown as cumulative distributions. (F) The average turning angle for each group was not significantly different from zero, nor was there a significant difference between them. (G, H) Example growth cone trajectories traced from the projected images of individual axons. Once initiated, growth cones travelled in mostly straight trajectories under both conditions. Several growth cones were often present on a single axon. Overlaid circles in the same colors as the growth cone tracts denote where tracts terminated. (I) The average number of growth cones per axon was unchanged by TTX. Scale bar is 5 μm.

(TTX -0.19 ± 0.14, Controls -0.19 ± 0.13, $p = 0.99$). Within the two groups, the switch of the branching ratio after the target was reached was significant for both controls (Control branch ratio before target 0.11 ± 0.09; Control branch ratio after target -0.19 ± 0.13, $p = 10-5$) and TTX treated larvae (TTX branch ratio before target 0.18 ± 0.098; TTX branch ratio after target -0.19 ± 0.14, $p = 10-5$) [Fig. 4(F), last four measures]. The branch ratio was not affected by the activity loss.

The speed of growth cone advancement was measured to see if the average velocity was affected by TTX. The distributions of the velocities were not normal (Shapiro–Wilks test). Controls travelled with a median speed of 12.6 μm/h and in TTX treated conditions the growth cones moved with a similar median speed of 11.2 μm/h, which was not significantly different from controls (Mann–Whitney U test, $p = 0.40$) [Fig. 5(A,B,C)]. The average turning angles of each growth cone are displayed in Figure 5(D,E).

Turning angles were defined as the angular difference in vector movement between successive movie frames. Angles were defined as positive if the turn was toward the target arborization zone and negative if it was away from the target.

An average turning angle was calculated for each growth cone. The distribution of average turning angles was not normal. The growth cones in control conditions had a median turning angle of 1.2° and in TTX treated conditions, the median turning angle

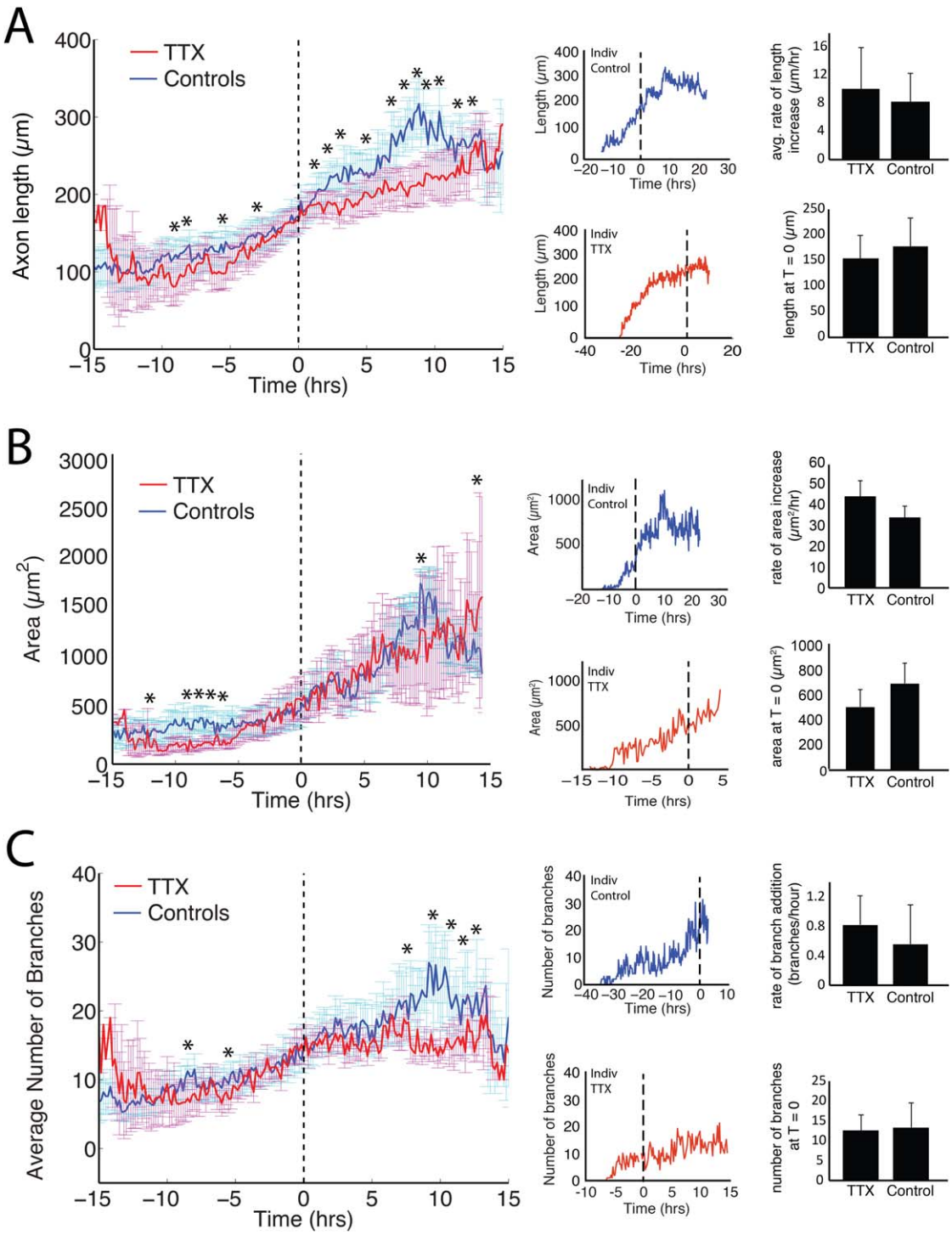

Figure 6.

was 2.0°, which were similar between groups (Mann–Whitney, $p = 0.48$) [Fig. 5(F)]. In both cases the majority of growth cones grew in almost entirely straight paths and TTX did not significantly alter the results. Although the average angles were small, they were significantly different from zero (Wilcoxon one-sample signed rank test, TTX, $p < 0.0001$; Controls, $p < 0.0001$). We then examined the individual growth cones in each sample to study their turning angles over their lifetimes, to examine if individual axons had an overall trajectory toward or away from the target. In both cases, no growth cones in control ($n = 33$) or TTX ($n = 39$) conditions had individual turning angles that were different from zero over their lifetimes (one sample t test, Wilcoxon one-sample signed test as appropriate given the distribution of angles/growth cone lifetime). The trajectories of growth cones on two representative axons (multiple growth cones can be present at the same or sequential times on a single, branching axon) are displayed in Figure 5(G,H). We also determined whether the number of growth cones per axon changed with TTX treatment. On average, control axons extended a median of 2.5 growth cones and TTX treated axons extended 3.0 growth cones, which was not significantly different (Mann–Whitney, $p = 0.49$) (Figure 5(I)).

We then determined whether other aspects of axon growth and pathfinding differed after treatment with TTX (Fig. 6) focusing on the length of the arbors, the area covered and the number of branches over time.

We examined whether the overall length of each axon was increased or decreased by TTX by examining the sum of the length of all branches over time [Fig. 6(A)]. Similar to the measures of branch ratio in Figure 4(F), first the slope and intercept of the individual axon measurements were calculated and compared with regard to length over time. Between the groups there was no difference in the rate of change of length (TTX 10.1 ± 4.0 μm/h; Controls 8.3 ± 5.8 μm/h, $p = 0.42$) or the average length when the target was reached (TTX 154 ± 46 μm, Controls 177 ± 55 μm, $p = 0.31$) (Bar graphs at left of Figure 6(A); mean ± SEM).

The averages at the six time points recorded in each hour were then compared between the two conditions. These groups of six points were normally distributed (Shapiro–Wilks test, $p > 0.05$) in the vast majority of cases (157/168). To be conservative a Bonferroni multiple comparisons correction was not applied to the normality test: if it had all groups would have passed the normality test. For normally distributed groups a Student's t test was used to compare between conditions. For the remaining 11 groups that failed the normality test we instead used a Mann–Whitney U test. We reviewed the raw numbers to determine if the non-normal distributions appeared at times of rapid change in averages over the hour that could skew the distribution, however, we found that they mostly occurred when the averages held to rather similar values for the hour. To reduce the potential for false positives in significance over multiple comparisons (as the period of imaging spanned 28 h), the Bonferroni correction was applied to both the t test and Mann–Whitney U test. During pathfinding, controls had significantly longer axon lengths at 3, 6, 9, and 10 h before the target was reached ($p \leq 0.001$ for

Figure 6 Differences between growth patterns of TTX and control axons. For the grouped data, comparisons were made between the conditions over each hourly interval. Stars mark hours where the measures were significantly different ($p < 0.0018$). (A) While pathfinding, the axons' total lengths (sum of all branches and primary axon shaft) were mostly similar between control and TTX groups. There were occasional hours when controls had more length than TTX treated axons during pathfinding but this was not consistent for long periods of time. After the target was reached (vertical dashed line at $t = 0$) the controls underwent a period of extension followed by a reduction in overall length. During this time they had significantly more length, while the TTX group maintained a slow but steady rate of length increase. The difference in length disappeared after 14 h at the target due to the differences in growth patterns. (B) Branches of control axons covered more area during pathfinding. After the target was reached, the control axons expanded and retracted, with TTX area steadily increasing. (C) Axons in the control and TTX treated groups had similar numbers of branches during pathfinding with a few hours where controls had more branches. In controls, the branch numbers increased as the axons elaborated an arbor with a period of significantly more branches from 8–13 h after the target was reached. Ten axons were included in each grouped panel. Individual example traces follow. Bar graphs represent the mean and SEM of the fit to a straight line for each axon, averaged by group, and displaying both rate of change and value on reaching the target for each measure in (A–C).

each hour). After the target was reached, the dynamics changed more markedly. Comparisons made at 2, 3, 5 h, and at every hour between 7–13 h after reaching the target, showed that controls were longer than TTX treated axons ($p < 0.001$ at every hour). By 14 h, there were no longer significant differences between the conditions [Fig. 6(A)].

Similarly, we looked at the area covered by a convex polygon drawn with corners at every branch tip [Fig. 6(B)]. When fitted to a straight line, the average area covered by the axons increased at similar rates (TTX 44 ± 8 μm2/h; Controls 34 ± 5 μm2 /h, $p = 0.31$). By this measure, the area covered as the target was reached was not altered by TTX treatment (TTX 514 ± 140 μm2, Controls 704 ± 166 μm2, $p = 0.39$) (Bar graphs at left of Figure 6(B); mean ± SEM). The overall trends hide differing temporal patterns, however. The averages of area covered at each time point were again combined into hourly segments and these segments compared between control and TTX environments. For several hours during the pathfinding stage control axons cover more area than TTX treated axons. At 12, 9, 8, 7, and 6 h before the target was reached the difference in area was statistically significant ($p < 0.001$ at every individual hour). After reaching the target, the control arbors expanded and retracted while TTX treated arbors continue to expand steadily, but more slowly. The control arbor expansions results in the controls gaining significantly larger area than the TTX treated arbors at 9 h after reaching the target ($p < 0.001$). However, due to the subsequent reduction in area, by 14 h the control arbors covered significantly less area than those treated with TTX, which had continued to expand ($p < 0.001$).

The average number of branches over time had similar rates of addition (TTX 0.82 ± 0.40 branches/h, Controls 0.56 ± 0.53 branches/h, $p = 0.22$). At the time the axons reached the target zone there were similar numbers of branches present in each case (TTX 12.5 ± 4.0, Controls 13.4 ± 6.1, $p = 0.73$) (Bar graphs at left of Figure 6(C); mean ± SEM). When the averages of each group were compared from hour to hour, control axons had more branches than TTX treated axons 8, 10, 11, 12, and 13 h after reaching the target ($p < 0.001$). The number of branches on TTX treated axons steadily increased from the time the target was reached until 14 h afterward. Controls had a sharper increase in number after reaching the target. At 14 h after the target was reached, there were no significant differences between the number of branches in control or TTX treated conditions. Before reaching the target there was no overall trend. However, for brief periods at 9 and 6 h before the target was reached controls had significantly more branches ($p < 0.001$).

DISCUSSION

The role of activity in initial axon pathfinding is controversial. Here, we investigated this question by injecting TTX into developing zebrafish to inhibit neural activity. Stuermer et al. (1990) previously showed that RGC axons arborize in the correct general area even with TTX treatment. The final arbor locations were topographic, even when segments of the retina (and the output axon generating RGCs) were removed to leave large portions of the tectum devoid of connections. Our work provides a complementary quantitative analysis of growth patterns and guidance in individual RGCs as they navigate an environment without neural activity.

During development, addition and deletion of branches occurs concurrently rather than as a period of overgrowth followed by refinement (Ruthazer et al., 2003). Time-lapse movies where images are taken every hour do not capture many of the more rapid dynamics and could conceal differences in growth or guidance mechanisms, despite a maintenance of overall topography. Similarly, movies that focus with high temporal frequency over a small period of time do not capture the changes that take place over longer periods of development. Here, we balanced these constraints and quantitatively described the changes to pathfinding behavior of RGCs with 10 min resolution from 2.5 to 4 dpf when challenged with TTX. While most aspects of branch and growth cone dynamics were robust to activity loss, we found measures in the initial pathfinding that do show change, especially in the extent of area covered by the branches during pathfinding.

Growth cone guidance and branching are both important features of retinotectal axon guidance in zebrafish and we hypothesized that a loss of activity might have changed the relative importance of the two methods. However, analysis of growth cone movements showed no difference between TTX and control conditions (Fig. 5), with velocities, turning angles, and trajectories remaining similar between the two groups. While branching was previously described as a rare event (Kaethner and Stuermer, 1994), dynamic and continual branching has now been recorded and implicated in zebrafish RGC guidance behaviors (Simpson et al., 2013). One aspect of branching important for guidance is the maintenance of biased branches; where more branches are directed

toward the target. This guidance ratio was also unaffected by the loss of activity (Fig. 4). Thus the two major forms of guidance do not depend on global activity.

We next turned to quantitative description of the patterns of growth in both pathfinding and early arborization to both enhance existing qualitative studies and also to determine if there were differences in the manner in which axons grow when their environments are silent. In our work, we see for the first time that the branches cover less area when pathfinding in a silenced environment (Fig. 6). The control axons showed brief periods during pathfinding where their length and number of branches briefly reached significantly higher levels than TTX treated axons, however, area was the only measure that remained consistently different during sequential measurements in the pathfinding phase.

Synapses have been linked to branch formation (e.g., Cline, 2001; Hutson and Chien, 2002; Meyer and Smith, 2006; Uesaka et al., 2006; Ruthazer et al., 2006; Hörnberg et al., 2013). Synapses provide a physical location for the extension of new branches and their presence on branches is a stabilizing influence (Meyer and Smith, 2006). The first synaptic puncta are present in zebrafish at 3 dpf (Meyer and Smith, 2006) and visual responses start at 68–79 hpf (Easter and Nicola, 1996). These ages cover times when the first pioneer axons are arborizing and also when the following waves of axons are growing in and pathfinding. No studies so far have looked for retinotectal synapses at earlier time points. The earliest synapses may be used to stabilize branches in pathfinding and support longer extensions. Without activity, the synapses may not be maintained, leading to shorter branches that cover less total area.

Axonal morphology becomes more affected by activity at later stages of arborization when synaptic communication between RGCs and tectal neurons likely mediates the formation of functional connections, and therefore the structure of the RGC arbor. After reaching the target, we observed the area of control axons expanded and contracted, which was not seen in the TTX treated arbors. In general, we found that controls had a greater length and higher numbers of branches, but by the last time point, they covered less area. The differences between the two groups was most apparent after approximately 10 h on the target (Fig. 6) when control axons had more length, area, and branches, with length and branch measurements remaining significantly higher than TTX treated axons as the area decreased, suggesting a steep increase in arbor density at that time that was blocked by TTX. However, as length and branch number lose significance at the end of our imaging period, the density may not have been maintained for long and may have been an intermediate step in finding the correct tectal synaptic partners.

To more fully understand how the the TTX is affecting the structure of the axons, our results can be compared to other studies on activity and arborization. In the *Mao* zebrafish mutant (Gnuegge et al., 2001) RGCs lose activity at 4–6 dpf. The arbor areas, or projection fields, were enlarged in these mutants but showed no significant increase in the length of individual axons. The branches were fewer and longer. In their study, this mutant phenotype could be phenocopied with TTX. Our analysis used the time that the center of the arbour's mass ceased to move forward as the time that the target was reached. This was a useful way to align axons which may grow into the tectum many hours apart, when time relative to dpf would be inappropriate. By the last time points in our study, approximately 4–4.5 dpf depending on the axon, we confirmed that TTX treated arbors were larger than controls but the sums of the branch lengths were similar and quantitatively showed how these measures change over early arborization.

Branches are often eliminated when correlated activity is not found. This process is rapid, and can take place in the 20 min following a change in synchronicity between two cells (Munz et al., 2014). Postsynaptic N-methyl-D-aspartate (NMDA) receptors detect correlated activity between partner neurons (Paoletti et al., 2013). Selective branch elimination can be blocked using NMDA antagonists (Ruthazer et al., 2003). However, the blockade has other effects as well the rate of branch additions increases and the lifetime of branches becomes shortened (Rajan et al., 1999). There are more rearrangements and a decrease in synapse stability (O'Rourke et al., 1994). Injecting TTX into *Xenopus* at later arborization stages also increases the rate of addition and elimination of branches and disrupts long term branch stability (Cohen-Cory, 1999). This impaired ability to correlate activity was not as important earlier in development. Blocking NMDA receptors in zebrafish from 2–4 dpf did not have effects on the number of branches, the rate of addition and deletion of branches, or branch lifetime, but did cause larger arbor areas with an increased distance between branches (Schmidt et al., 2000), similar to what we and others have seen at 4–5 dpf.

The dynamic nature of our measures leads us to suggest that the exact time of analysis, especially in relation to activity and growth, is a crucial element when discussing the effects of perturbing normal zebrafish development. Events such as the switch in RGCs from

embryonic to adult forms of sodium channels (Gnuegge et al., 2001), and a growing need to compete for space to both form physical synapses and receive nerve growth factors for survival (e.g., brain-derived neurotrophic factor (BDNF)) released from postsynaptic partners, may make activity even more important at later stages of arbor development.

Treatment with TTX silences electrical activity in both the ingrowing axons and the dendrites of the target cells in the tectum. A remaining question is whether matched activity is important for guidance, as global inhibition could mask an effect that would be present when either partner was silenced alone. There are contradictory results present in the literature for the arbor dynamics at later ages. Silencing a single zebrafish RGC axon with tetanus toxin resulted in increased branch outgrowth at 7 dpf, such that the one arbour ends up occupying a larger area (Fredj et al., 2010). This increase in area agreed with what we saw during the arborization period. While silenced at 7 dpf, axons also displayed highly dynamic, short lived filopodia, which are characteristic of immature axons (Fredj et al., 2010) and agreed with the structures observed in our 'immature' pathfinding axons. Further experiments by Fredj et al. (2010) showed that this was a competitive process, as when other cells nearby were also silenced, the effect disappeared. Conversely, a separate study found growth inhibition and decreased branch formation at 5 dpf in axons with activity suppressed by an over expression of either the potassium channel Kir2.1 or a dominant negative SNARE protein preventing the release of neurotransmitters (Hua et al., 2005). When using TTX, as in our study, Hua et al. found no difference in arbor length or branch number in larvae without activity compared to controls, consistent with our results at the last time-points measured.

Thus, at least for zebrafish retinotectal map development, the role of activity is not clearly segregated into two time periods. While activity is critically important for axon rearrangements and map refinement once axons have made initial contact with their targets, it also plays a small role in the dynamics of axon pathfinding to that point. However, guidance and branching, including the branch ratio during pathfinding, appears to be informed only by molecular cues.

ACKNOWLEDGMENTS

The authors thank Andrew Thompson for the use of his HuC:GCaMP5 zebrafish embryos, and Richard Faville, David Reynolds, and Kelsey Chalmers for their work on the Matlab analysis program, and the reviewers for their helpful suggestions.

REFERENCES

Akerboom J, Chen TW, Wardill TJ, Tian L, Marvin JS, Mutlu S, Caldern NC, et al. 2012. Optimization of a gcamp calcium indicator for neural activity imaging. J Neurosci 32:13819–13840.

Catalano SM, Shatz CJ. 1998. Activity-dependent cortical target selection by thalamic axons. Science 281:559–562.

Cline HT. 2001. Dendritic arbor development and synaptogenesis. Curr Opin Neurobiol 11:118–126.

Cohen-Cory S. 1999. BDNF modulates, but does not mediate, activity-dependent branching and remodeling of optic axon arbors in vivo. J Neurosci 19:9996–10003.

Easter JS, Nicola GN. 1996. The development of vision in the zebrafish (danio rerio). Dev Biol 180:646–663.

Fraser SE, O'Rourke NA. 1990. In situ analysis of neuronal dynamics and positional cues in the patterning of nerve connections. J Exp Biol 153:61–70.

Fredj NB, Hammond S, Otsuna H, Chien CB, Burrone J, Meyer MP. 2010. Synaptic activity and activity-dependent competition regulates axon arbor maturation, growth arrest, and territory in the retinotectal projection. J Neurosci 30:10939–10951.

Garel S, López-Bendito G. 2014. Inputs from the thalamocortical system on axon pathfinding mechanisms. Curr Opin Neurobiol 27C:143–150.

Gaze RM, Keating MJ, Ostberg A, Chung SH. 1979. The relationship between retinal and tectal growth in larval xenopus: implications for the development of the retinotectal projection. J Embryol Exp Morphol 53:103–143.

Gnuegge L, Schmid S, Neuhauss SC. 2001. Analysis of the activity-deprived zebrafish mutant macho reveals an essential requirement of neuronal activity for the development of a fine- grained visuotopic map. J Neurosci 21: 3542–3548.

Harris WA. 1984. Axonal pathfinding in the absence of normal pathways and impulse activity. J Neurosci 4:1153–1162.

Hörnberg H, Wollerton-van Horck F, Maurus D, Zwart M, Svoboda H, Harris WA, Holt CE. 2013. Rna-binding protein hermes/rbpms inversely affects synapse density and axon arbor formation in retinal ganglion cells in vivo. J Neurosci 33:10384–10395.

Hua JY, Smear MC, Baier H, Smith SJ. 2005. Regulation of axon growth in vivo by activity- based competition. Nature 434:1022–1026.

Hutson LD, Chien CB. 2002. Pathfinding and error correction by retinal axons: The role of astray/robo2. Neuron 33:205–217.

Kaethner RJ, Stuermer CA. 1992. Dynamics of terminal arbor formation and target approach of retinotectal axons in living zebrafish embryos: A time-lapse study of single axons. J Neurosci 12:3257–3271.

Kaethner RJ, Stuermer CA. 1994. Growth behavior of retinotectal axons in live zebrafish embryos under TTX-

induced neural impulse blockade. J Neurobiol 25:781–796.

Karlsson J, von Hofsten J, Olsson PE. 2001. Generating transparent zebrafish: a refined method to improve detection of gene expression during embryonic development. Mar Biotechnol (NY) 3:522–527.

Kirkby LA, Sack GS, Firl A, Feller MB. 2013. A role for correlated spontaneous activity in the assembly of neural circuits. Neuron 80:1129–1144.

Kita EM, Scott E, Goodhill G. 2014. Topographic wiring of the retinotectal connection in zebrafish. Dev Neurobiol, DOI: 10.1002/dneu.22256

Kobayashi T, Nakamura H, Yasuda M. 1990. Disturbance of refinement of retinotectal projection in chick embryos by tetrodotoxin and grayanotoxin. Brain Res Dev Brain Res 57:29–35.

Lister JA, Robertson CP, Lepage T, Johnson SL, Raible DW. 1999. Nacre encodes a zebrafish microphthalmia-related protein that regulates neural-crest-derived pigment cell fate. Development 126:3757–3767.

McLoon SC. 1985. Evidence for shifting connections during development of the chick retinotectal projection. J Neurosci 5:2570–2580.

Meyer MP, Smith SJ. 2006. Evidence from in vivo imaging that synaptogenesis guides the growth and branching of axonal arbors by two distinct mechanisms. J Neurosci 26: 3604–3614.

Ming G, Henley J, Tessier-Lavigne M, Song H, Poo M. 2001. Electrical activity modulates growth cone guidance by diffusible factors. Neuron 29:441–452.

Munz M, Gobert D, Schohl A, Poqurusse J, Podgorski K, Spratt P, Ruthazer ES. 2014. Rapid hebbian axonal remodeling mediated by visual stimulation. Science 344: 904–909.

O'Rourke NA, Cline HT, Fraser SE. 1994. Rapid remodeling of retinal arbors in the tectum with and without blockade of synaptic transmission. Neuron 12:921–934.

Paoletti P, Bellone C, Zhou Q. 2013. Nmda receptor subunit diversity: impact on receptor properties, synaptic plasticity and disease. Nat Rev Neurosci 14:383–400.

Park HC, Kim CH, Bae YK, Yeo SY, Kim SH, Hong SK, Shin J, et al. 2000. Analysis of upstream elements in the huc promoter leads to the establishment of transgenic zebrafish with fluorescent neurons. Dev Biol 227:279–293.

Rajan I, Witte S, Cline HT. 1999. Nmda receptor activity stabilizes presynaptic retinotectal axons and postsynaptic optic tectal cell dendrites in vivo. J Neurobiol 38:357–368.

Reh TA, Constantine-Paton M. 1984. Retinal ganglion cell terminals change their projection sites during larval development of rana pipiens. J Neurosci 4:442–457.

Rodger J, Mo C, Wilks T, Dunlop SA, Sherrard RM. 2012. Transcranial pulsed magnetic field stimulation facilitates reorganization of abnormal neural circuits and corrects behavioral deficits without disrupting normal connectivity. FASEB J 26:1593–1606.

Ruthazer ES, Akerman CJ, Cline HT. 2003. Control of axon branch dynamics by correlated activity in vivo. Science 301:66–70.

Ruthazer ES, Cline HT. 2004. Insights into activity-dependent map formation from the retino- tectal system: a middle-of-the-brain perspective. J Neurobiol 59:134–146.

Ruthazer ES, Li J, Cline HT. 2006. Stabilization of axon branch dynamics by synaptic matura- tion. J Neurosci 26: 3594–3603.

Schmidt JT, Buzzard M, Borress R, Dhillon S. 2000. MK801 increases retinotectal arbor size in developing zebrafish without affecting kinetics of branch elimination and addition. J Neurobiol 42:303–314.

Scott EK, Mason L, Arrenberg AB, Ziv L, Gosse NJ, Xiao T, Chi NC, et al. 2007. Targeting neural circuitry in zebrafish using GAL4 enhancer trapping. Nat Methods 4: 323–326.

Simpson HD, Kita EM, Scott EK, Goodhill GJ. 2013. A quantitative analysis of branching, growth cone turning, and directed growth in zebrafish retinotectal axon guidance. J Comp Neurol 521:1409–1429.

Spitzer NC. 2006. Electrical activity in early neuronal development. Nature 444:707–712.

Sretavan DW, Shatz CJ, Stryker MP. 1988. Modification of retinal ganglion cell axon morphology by prenatal infusion of tetrodotoxin. Nature 336:468–471.

Stuermer CA. 1988. Retinotopic organization of the developing retinotectal projection in the zebrafish embryo. J Neurosci 8:4513–4530.

Stuermer CA, Raymond PA. 1989. Developing retinotectal projection in larval goldfish. J Comp Neurol 281:630–640.

Stuermer CA, Rohrer B, Münz H. 1990. Development of the retinotectal projection in zebrafish embryos under TTX-induced neural-impulse blockade. J Neurosci 10: 3615–3626.

Suàrez R, Fenlon LR, Marek R, Avitan L, Sah P, Goodhill GJ, Richards LJ. 2014. Balanced interhemispheric cortical activity is required for correct targeting of the corpus callosum. Neuron 82:1289–1298.

Sumbre G, Poo MM. 2013. Monitoring tectal neuronal activities and motor behavior in zebrafish larvae. Cold Spring Harb Protoc 2013:873–879.

Uesaka N, Ruthazer ES, Yamamoto N. 2006. The role of neural activity in cortical axon branching. Neuroscientist 12:102–106.

Xu HP, Furman M, Mineur YS, Chen H, King SL, Zenisek D, Zhou ZJ, et al. 2011. An instructive role for patterned spontaneous retinal activity in mouse visual map development. Neuron 70:1115–1127.